Supporting Information

Interfacial Halogen Bonding Probed by Force Spectroscopy

Meital Boterashvili,[a] Tanya Shirman,[a] Sidney R. Cohen,[b] Guennadi Evmenenko,[c] Pulak Dutta,[c] Petr Milko,[b] Gregory Leitus,[b] Michal Lahav,[a] and Milko E. van der Boom *[a]

[a]*Departments of Organic Chemistry and* [b]*Chemical Research Support, The Weizmann Institute of Science, Rehovot 76100, Israel.* [c]*Department of Physics and Astronomy, Northwestern University, Evanston, Illinois 60208-3113, United States.* E-mail: milko.vanderboom@weizmann.ac.il

Materials and methods. 11-Cyanoundecyltrichlorosilane (Gelest), 3-iodo-*n*-propyl-1-trimethoxysilane (Sigma Aldrich), 2,7-di-*tert*-butyl-9,9-dimethyl-xanthene (Sigma Aldrich), formaldehyde (37%, J.T. Baker), and iodomethane (Fluka) were used as received. THF and pentane were dried by distillation from Na, degassed, and stored in an N_2-filled M. Braun glove box (H_2O and O_2 levels <2 ppm). Hexane (AR grade; BioLab), acetone (Mallinckrodt Baker), and ethanol (Merck) were used as received. Compounds **5** and **9** were prepared according to published procedures.[S1,S2] All glassware used for monolayer formation was cleaned with a piranha solution (7:3 v/v H_2SO_4/30% H_2O_2) for 1 h. ***Caution: piranha solution is an extremely dangerous oxidizing agent and should be handled with care using appropriate personal protection.*** Subsequently, the glassware was rinsed repeatedly with deionized (DI) water and dried for at least 2 h at 130°C. Single-crystal Silicon (100) substrates (Wafernet; 1 cm × 2 cm) were cleaned by sequential sonication (8 min each) in hexane, acetone, and ethanol. The substrates were then dried under an N_2 stream. Subsequently, they were exposed to UV/ozone treatment for 20 min in a UVOCS cleaning system (Montgomery, PA). Then, the substrates were rinsed with ethanol (3×) and immersed in ethanol for at least 10 min. The substrates were then dried under an N_2 stream and dried for 2 h at 130°C. Quartz slides (Chemglass, Inc.; 0.8 cm × 2.5 cm) were rinsed with DI water followed by immersion in a piranha solution (7:3 v/v H_2SO_4/30% H_2O_2) for 1 h. Subsequently, the substrates were rinsed with DI water followed by the RCA cleaning protocol: 1:5:1 (v/v/v) NH_4OH/H_2O/30% H_2O_2 at rt for 1 h. The substrates were washed with DI water, rinsed with ethanol (3×), and immersed in ethanol for at least 10 min. The substrates were then dried under an N_2 stream and dried for 2 h at 130°C. MSNL AFM tips (Bruker; Santa Barbara, CA) for force spectroscopy measurements were cleaned according to the abovementioned cleaning protocol used for silicon substrates, without the sonication in hexane, acetone, and ethanol. ^{1}H, ^{13}C{^{1}H}, and ^{19}F{^{1}H} NMR spectra were recorded on a Bruker Avance 300 NMR spectrometer, a Bruker Avance 400 NMR spectrometer, or a Bruker Avance 500 NMR spectrometer. All chemical shifts (δ) are reported in ppm and coupling constants (J) are in Hz. The ^{1}H and ^{13}C{^{1}H} NMR chemical shifts are reported relative to TMS or to residual solvent peaks. Mass spectrometry (MS) was carried out using a micromass ZQ 4000 mass spectrometer. High-resolution mass spectrometry (HRMS) was carried out using a SYNAPT high-definition Q-TOF mass spectrometer manufactured by Waters-Micromass (Manchester, U.K.). Elemental Analysis was performed by H. Kolbe, Mikroanalytisches Laboratorium, Mülheim an der Ruhr, Germany. UV/Vis spectra were recorded using Varian Cary 100 or 500 spectrophotometers (in double beam transmission mode). The film thickness was estimated using an M 2000V (J. A. Woollam Co., Inc.) ellipsometer with VASE32 software. Measurements were performed on modified silicon substrates for each 2 degrees at a range of 65º-75º over wavelengths of 399-1000 nm. Parameters A, B, and C were 1.45, 0.01, and 0.00, respectively, with MSE < 10 for a Cauchy model. The SiO_2 layer was calibrated to be 17 Å. Atomic force microscopy (AFM) images of the modified silicon substrates were recorded using a Solver P47 (NT-MDT, Russia) operating in semicontact mode, using AV240 AFM probes (Olympus) with a resonant frequency of 70-90 kHz. Images were taken at different fields of view (0.5-5 μm) to ensure reproducibility. The roughness values, R_q, were obtained from 1 μm × 1 μm images. X-ray photoelectron spectroscopy (XPS) measurements were carried out on modified silicon substrates with the Kratos AXIS ULTRA system using a monochromatized Al Kα X-ray source ($h\nu = 1486.6$ eV) at 75 W and with detection pass energies ranging between 10 and 80 eV. Angular resolved spectra were recorded at $\theta = 0°$ (normal), 55.0°, and 65.0°, where θ is the take-off angle with respect to the surface normal. X-ray reflectivity (XRR) measurements were carried out on modified silicon substrates at beam lines X6B and X18A of the National Synchrotron Light Source, Brookhaven (Upton, NY) using a Huber four-circle diffractometer in the specular reflection mode (i.e., the incident angle is equal to the exit angle θ). X-rays of energy E = 10 keV (λ = 1.24 Å) were used for these measurements. The beam size was 0.3-0.4 mm vertically and 0.5 mm horizontally. The resolution was 3×10^{-3} $Å^{-1}$. The samples were placed under helium during measurements to reduce background scattering and radiation damage. The sample preparation and the XRR measurements were performed at ambient laboratory temperature, which ranged from 20 to 25ºC. Scanning electron microscopy (SEM) images were obtained from a Leo Supra 550 SEM or Ultra 55 SEM with secondary electron detectors, operating at 3 kV. Force-distance (FD) curves were obtained using an NTEGRA AFM (NT-MDT, Zelenograd, Russia) with a liquid cell. Each surface-tip combination was measured at several contact points with ~50 FD curves taken at each point. The measurements were performed in liquid media, to avoid capillary effects, using MSNL tips treated as described above. The force constant of the cantilevers was determined with a MultiMode AFM instrument (Bruker; Santa Barbara, CA) using an E scanner and Nanoscope V electronics, and applying the thermal noise calibration provided in the Nanoscope software. Measurements in ethanol were performed with cantilever E (nominal force constant 0.175 ± 0.018 N/m) and measurements in hexane were performed with cantilever B or D (nominal force constant 0.027 ± 0.003 N/m and 0.045 ± 0.005 N/m, respectively). Forces were calculated taking into account the corresponding spring constant.

Computational details. All calculations were carried out using Gaussian 09 Revision C.01.[S3] The M06-2X functional[S4] was used to optimize structures. It is a meta-hybrid functional containing 54% HF exchange and was shown to be a suitable functional to describe weak interactions, π–π stacking, and halogen bonds.[S4-S5] A combined basis set was used with the M06-2X functional, specifically the Jensen's polarization consistent triple-ζ basis set (pc-2)[S6] on the main group elements and the Stuttgart-Dresden (SDD) basis set with a relativistic effective core potential (RECP) on the iodine atoms.[S6d,e] Frequency calculations at the same level of theory as the geometry optimization confirmed that the optimized structures are local minima by the absence of imaginary frequencies. Single-point energy calculations of the optimized structures were done using the DSD-PBEP86 double-hybrid functional by Kozuch and Martin[S7] in conjunction with the combined basis set. DSD-PBEP86 is a double-hybrid functional incorporating Perdew-Burke-Ernzerhof (PBE)[S8] DFT exchange with "exact" Hartree-Fock exchange, the Perdew-86 correlation with "exact" spin-component scaled[S9] second-order Møller-

Plesset[S10] (SCS-MP2) correlation and a dispersion correction[S11] - specifically Grimme's third version of his empirical dispersion correction (DFTD3)[S11d,S12] with Becke-Johnson (BJ) dampening.[S12,S13] Bulk solvation effects were modeled using the SMD model derived by Marerich et al.,[S14a] which is an empirical reparametrization at the polarized-continuum model.[S14b,c] Partial atomic charges were obtained using CM5PAC, which is Charge Model 5 yielding class IV atomic charges derived from the Hirshfeld population analysis.[S15] The NCIPLOT program, which was developed by Contreras-García et al., was used to identify and visualize non-covalent interactions.[S16] It analyzes the reduced density gradient s of the electron density ρ obtained by the single-point energy calculations at low densities. In our study, wavefunctions obtained at the M06-2X level of theory were analyzed. The selected basis set was the standard Pople basis set triple-ζ quality with polarization functions on all elements (6-311G**).[S17] Our version of NCIPlot has been locally modified to allow for *f*-functions and parallelization using MPI.

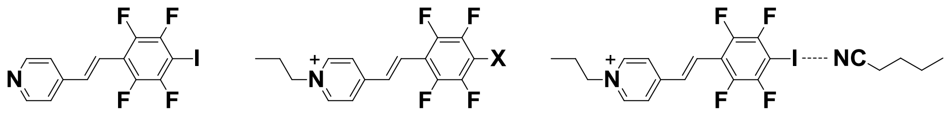

5

6: X = I
7: X = F

8

Scheme S1 Molecular structures of compounds **5**-**7** and complex **8**, studied by DFT calculations.

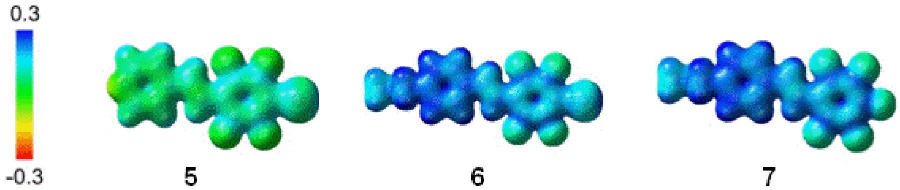

5 6 7

Fig. S1 Gas-phase electron density distribution mapped with electrostatic potential (in atomic units; blue is the most positive and red is the most negative) for compounds **5**-**7**.

Table S1 CM5 partial group charges for compounds **5-7** and complex **8** (Scheme S1).

Solvent	Structure	XF_4C_6	-CH=CH-	$-C_5H_4N-$	$-C_3H_7$	C_{para}[1]	X	C–X	CN	$-C_4H_9$
gas-phase	C_4H_9CN								-0.18	0.18
	5 (X=I)	-0.03	0.03	0.00		-0.03	0.01	-0.02		
	6 (X=I)	0.10	0.09	0.45	0.35	-0.03	0.10	0.07		
	7 (X=F)	0.10	0.09	0.46	0.35	0.14	-0.08	0.05		
	8 (X=I)	0.02	0.09	0.44	0.35	-0.04	0.07	0.03	-0.12	0.22
n-hexane	C_4H_9CN								-0.20	0.20
	6 (X=I)	0.06	0.10	0.49	0.35	-0.04	0.09	0.05		
	7 (X=F)	0.06	0.10	0.49	0.35	0.13	-0.09	0.04		
	8 (X=I)	-0.02	0.09	0.48	0.35	-0.04	0.05	0.01	-0.13	0.22
ethanol	C_4H_9CN								-0.23	0.23
	6 (X=I)	0.01	0.10	0.53	0.35	-0.04	0.07	0.03		
	7 (X=F)	0.02	0.10	0.53	0.35	0.13	-0.11	0.02		
	8 (X=I)	-0.08	0.10	0.53	0.35	-0.05	0.01	-0.04	-0.14	0.24

[1] C_{para} is the carbon atom bound to X.

Table S2 Reaction energies (kcal/mol) and N-I Wiberg bond index obtained in the formation of complex **8** (Scheme S1).

Solvent	$\Delta_r E^{SCF}$	$\Delta_r E^{0K}$	$\Delta_r H^{298K}$	N-I Wiberg bond index
gas-phase	-9.2	-8.5	-8.8	0.0416
n-hexane	-6.4	-5.7	-5.0	0.0404
ethanol	-2.4	-1.7	-2.4	0.0392

Preparation of (*E*)-4-(2,3,5,6-tetrafluoro-4-iodostyryl)-1-(3-(trimethoxysilyl)-propyl)pyridin-1-ium iodide (1). In an N_2-filled glove box, an excess of 3-iodo-*n*-propyl-1-trimethoxysilane (580 μL, 2.96 mmol) was added to a dry THF solution (~25 mL) of chromophore **5** (93 mg, 0.25 mmol) in a side-arm flask. The reaction mixture was stirred and heated for 5 days at 80°C, resulting in the precipitation of a yellow powder. The solvent was removed with a pipette and the yellow product was washed repeatedly with THF and cold (-30°C) pentane, and was then dried under high vacuum, yielding chromophore **1** (59 mg, 35%). ^{1}H NMR (500 MHz, DMSO-d_6): δ (ppm) 9.03 (2H, d, $^3J_{HH} = 6.9$ Hz, pyr), 8.47 (2H, d, $^3J_{HH} = 6.9$ Hz, pyr), 7.81 (1H, d, $^3J_{HH} = 16.8$ Hz, CH=CH), 7.68 (1H, d, $^3J_{HH} = 16.7$ Hz, CH=CH), 4.49 (2H, t, $^3J_{HH} = 7.2$ Hz, CH_2-N), 3.47 (9H, s, $Si(OCH_3)_3$), 1.97 (2H, m, CH_2), 0.58 (2H, m, CH_2-Si). $^{13}C\{^1H\}$ NMR (500 MHz, DMSO-d_6): δ (ppm) 151.32 (s, C_q-pyr), 146.84 (dm, $^1J_{FC} = 239.5$ Hz, C-F), 144.65 (s, pyr), 143.8 (dm, $^1J_{FC} = 256.1$ Hz, C-F), 131.59 (m, CH=CH), 125.0 (m, CH=CH), 124.89 (s, pyr), 114.89 (m, Ar_F-C_q), 77.96 (m, C-I), 62.07 (s, CH_2-N), 50.08 (s, $Si(OCH_3)_3$), 24.44 (s, CH_2), 5.28 (s, CH_2-Si). $^{19}F\{^1H\}$ NMR (300 MHz, DMSO-d_6): δ (ppm) -123.0 (2F, dd, $^3J_{FF}$ = 24.3 Hz, $^4J_{FF}$ = 11.4 Hz, C-F), -140.06 (2F, dd, $^3J_{FF}$ = 24.3 Hz, $^4J_{FF}$ = 11.4 Hz, C-F). MS (ES^+) *m/z*: calcd. for $C_{19}H_{21}F_4INO_3Si^+$ 542.03; found 542.12. UV/Vis (THF): λ_{max}, nm (ε, cm^{-1} M^{-1}) = 334 (32×10^3).

Preparation of (*E*)-4-(2-(perfluorophenyl)vinyl)-1-(3-(trimethoxysilyl)propyl)-pyridin-1-ium iodide (2). In an N_2-filled glove box an excess of 3-iodo-*n*-propyl-1-trimethoxysilane (665 μL, 3.39 mmol) was added to a dry THF solution (~15 mL) of chromophore **9** (77 mg, 0.28 mmol) in a side-arm flask. The reaction mixture was stirred and heated for 5 days at 80°C. Subsequently, the volume was reduced to ~2 mL. Addition of cold (-30°C) pentane to the reaction mixture resulted in the precipitation of a yellow-brown powder. The solvent was removed with a pipette and the resulting powder was washed repeatedly with THF and cold (-30°C) pentane, and was then dried under high vacuum, yielding chromophore **2** (89 mg, 57%). ^1H NMR (300 MHz, DMSO-d_6): δ (ppm) 9.03 (2H, d, $^3J_{HH}$ = 6.8 Hz, pyr), 8.46 (2H, d, $^3J_{HH}$ = 6.8 Hz, pyr), 7.80 (1H, d, $^3J_{HH}$ = 16.8 Hz, CH=CH), 7.64 (1H, d, $^3J_{HH}$ = 16.8 Hz, CH=CH), 4.49 (2H, t, $^3J_{HH}$ = 7.2 Hz, CH_2-N), 3.47 (9H, s, $Si(OCH_3)_3$), 1.96 (2H, m, CH_2), 0.58 (2H, m, CH_2-Si). $^{13}C\{^1H\}$ NMR (500 MHz, DMSO-d_6): δ (ppm) 151.25 (s, C_q-pyr), 144.79 (dm, $^1J_{FC}$ = 251.9 Hz, C-F), 144.63 (s, pyr), 140.88 (dm, $^1J_{FC}$ = 254.4 Hz, C-F), 137.35 (dm, $^1J_{FC}$ = 249.1 Hz, C-F), 131.32 (m, CH=CH), 124.86 (s, pyr), 124.04 (s, CH=CH), 110.44 (m, Ar_F-C_q), 62.02 (s, CH_2-N), 50.07 (s, $Si(OCH_3)_3$), 24.44 (s, CH_2), 5.26 (s, CH_2-Si). $^{19}F\{^1H\}$ NMR (300 MHz, DMSO-d_6): δ (ppm) -141.17 (2F, dd $^3J_{FF}$ = 23.1 Hz, $^4J_{FF}$ = 6.0 Hz, C-F), -153.06 (1F, m, C-F), -163.02 (2F, m, C-F). MS (ES^+) *m/z*: calcd. for $C_{19}H_{21}F_5NO_3Si^+$ 434.12; found 434.14. UV/Vis (THF): λ_{max}, nm (ε, cm^{-1} M^{-1}) = 297 (31×10^3).

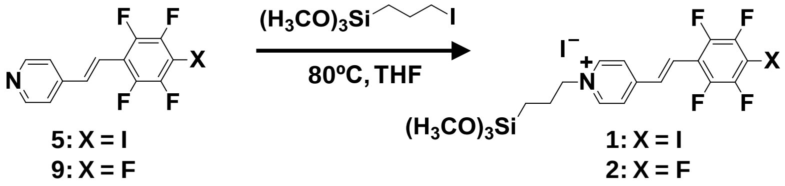

Scheme S2 Formation and molecular structures of compounds **1** and **2**.

Preparation of 2,7-di-*tert*-butyl-4,5-bis(chloromethyl)-9,9-dimethyl-9*H*-xanthene (11). Compound **11** was prepared using a procedure modified from the literature.[S18] 2,7-Di-*tert*-butyl-9,9-dimethyl-9*H*-xanthene (**10**; 1.6 g, 5.0 mmol) was dissolved in acetic acid (80 mL) under argon, followed by the addition of conc. HCl (20 mL) and formaldehyde (37%, 8 mL). The reaction mixture was heated to 70°C. Conc. H_2SO_4 (6.4 mL) was added dropwise. The reaction mixture was stirred overnight at 80°C. After rt was attained, H_2O (~50 mL) was added to the reaction mixture and the product was extracted with CH_2Cl_2 (3 × 100 mL). The organic extract was washed with an aqueous solution of $NaHCO_3$ and then with brine. The solvent was evaporated under reduced pressure, yielding compound **11** (1.9 g, 91%). ^{1}H NMR (300 MHz, $CDCl_3$): δ (ppm) 7.40 (2H, d, $^4J_{HH}$ = 2.3 Hz, Ar-H), 7.28 (2H, d, $^4J_{HH}$ = 2.3 Hz, Ar-H), 4.87 (4H, s, CH_2Cl), 1.64 (6H, s, CH_3), 1.34 (18H, s, *t*-butyl). MS (ES^+) *m/z*: calcd. for $C_{25}H_{32}Cl_2ONa^+$ 441.17; found 441.25, calcd. for $C_{25}H_{32}Cl_2OK^+$ 457.15; found 457.22.

Preparation of 2,7-di-*tert*-butyl-4,5-bis(iodomethyl)-9,9-dimethyl-9*H*-xanthene (**12**). Compound **11** (418 mg, 1.00 mmol) and an excess of sodium iodide (600 mg, 4.00 mmol) were suspended in 10 mL acetone under argon. The reaction was left stirring at rt for 7 days. The solvent was then evaporated under reduced pressure and the remaining solid was washed with water and filtered out, yielding compound **12** (290 mg, 48%). ^{1}H NMR (300 MHz, $CDCl_3$): δ (ppm) 7.35 (2H, d, $^4J_{HH}$ = 2.3 Hz, Ar-H), 7.24 (2H, d, $^4J_{HH}$ = 2.3 Hz, Ar-H), 4.79 (4H, s, CH_2I), 1.63 (6H, s, CH_3), 1.32 (18H, s, *t*-butyl). MS (ES^+) *m/z*: calcd. for $C_{25}H_{32}I_2ONa^+$ 625.04; found 625.11, calcd. for $C_{25}H_{32}Cl_2OK^+$ 641.02; found 641.15.

Preparation of compound 3. Compound **12** (76 mg, 0.13 mmol) and an excess of (*E*)-4-(2-(perfluorophenyl)vinyl)pyridine (**9**; 150 mg, 0.553 mmol) were dissolved in ~5 mL dry THF in a side-arm flask under N_2. The reaction was left stirring at 78°C for 20 h. The solvent was evaporated to ~1 mL and cold (-30°C) pentane was added, resulting in the precipitation of compound **3**. The solvent was removed with a pipette and the yellow precipitate was washed repeatedly with THF and cold (-30°C) pentane, and was then dried under high vacuum, yielding compound **3** (85 mg, 74%). ^{1}H NMR (300 MHz, DMSO-d_6): δ (ppm) 9.40 (4H, d, $^3J_{HH}$ = 5.9 Hz, pyr), 8.22 (4H, d, $^3J_{HH}$ = 6.3 Hz, pyr), 7.65 (2H, d, $^3J_{HH}$ = 16.7 Hz, CH=CH), 7.54 (4H, m, CH=CH + Ar-H), 6.95 (2H, d, $^4J_{HH}$ = 2.1 Hz, Ar-H) 6.48 (4H, s, CH_2-N), 1.72 (6H, s, CH_3), 1.29 (18H, s, *t*-butyl). ^{13}C NMR (400 MHz, $CDCl_3$): δ (ppm) 152.50 (C_q), 147.23 (C_q), 145.60 (C-F), 145.50 (C_q), 145.06 (C-H), 141.86 (C-F), 137.81 (C-F), 130.31 (C_q), 130.16 (C-H), 128.29 (C-H), 125.76 (C-H), 125.28 (C-H), 125.18 (C-H), 119.00 (C_q), 110.17 (C_q), 59.77 (CH_2-N), 34.65 (C_q), 34.60 (C_q), 32.99 (CH_3), 31.39 (CH_3). ^{19}F{^{1}H} NMR (300 MHz, $CDCl_3$): δ (ppm) -139.54 (4F, m, C-F), -150.57 (2F, m, C-F), -161.66 (4F, m, C-F). HRMS (ES$^+$) *m/z*: calcd. for $C_{51}H_{44}N_2OF_{10}I^+$ 1017.2339; found 1017.2333.

X-ray analysis of compound 3. Compound **3** was crystallized from $CDCl_3$ by slow evaporation at rt, affording crystals of **3**, manifested as orange crystals. *Crystal data***:** $C_{104}H_{90}Cl6F_{20}I_7N_4O_2$, orange plates, 0.01 × 0.05 × 0.05 mm^3, Triclinic, P-1 (N 2), a = 15.433(3) Å, b = 19.544(4) Å, c = 20.069(4) Å, α = 81.88(2)°, β = 77.72(4)°, γ = 68.69(3)°, from 20 degrees of data, T = 120(2) K, V = 5496.7(22) Å^3, Z = 2, F_w = 2908.8, D_c = 1.757 Mg·m^{-3}, μ = 2.205 mm^{-1}. *Data collection and processing*: Bruker Appex2 KappaCCD diffractometer, MoKα (λ = 0.71073 Å), graphite monochromator, 35209 reflections collected, $-19\leq h\leq 20$, $-23\leq k\leq 25$, $-26\leq l\leq 14$, frame scan width = 0.5°, scan speed 1.0° per 220 sec, typical peak mosaicity 0.88°, 24079 independent reflections (R_{int} = 0.0249). The data were processed with Apex2. *Solution and refinement*: The structure was solved by direct method SHELX-97. Full matrix least-squares refinement was based on F^2 with SHELX-97. 1315 parameters with 0 restraints, final R_1 = 0.0485 (based on F^2) for data with I>2σ (I) and R_1 = 0.0979 on 24079 reflections. Goodness of fit on F^2 = 1.040, the largest electron density peak = 2.150 e·Å^{-3}, the deepest hole = -1.108 e·Å^{-3}.

Preparation of (*E*)-1-methyl-4-(2-(perfluorophenyl)vinyl)pyridin-1-ium iodide (4). An excess of iodomethane (121 mg, 0.852 mmol) was added to a dry THF (1.5 mL) solution of chromophore **9** (58 mg, 0.21 mmol). The reaction mixture was stirred for 3 days at rt. The yellow precipitate (72 mg, 83% yield) was isolated as a powder using a Büchner funnel after washing with ~2 mL THF. ^{1}H NMR (300 MHz, $CDCl_3$): δ (ppm)

9.18 (2H, d, $^3J_{HH}$ = 6.7 Hz, pyr), 8.15 (2H, d, $^3J_{HH}$ = 6.8 Hz, pyr), 7.56 (1H, d, $^3J_{HH}$ = 16.6 Hz, CH=CH), 7.49 (1H, d, $^3J_{HH}$ = 16.9 Hz, CH=CH), 4.66 (3H, s, CH_3-N). $^{13}C\{^1H\}$ NMR (500 MHz, $CDCl_3$): δ (ppm) 151.99 (s; pyr, C_q), 145.72 (s; pyr), 145.49 (dm, $^1J_{FC}$ = 251.2 Hz; C-F), 141.88 (dm, $^1J_{FC}$ = 259.8 Hz; C-F), 137.83 (dm, $^1J_{FC}$ = 253.7Hz; C-F), 129.98 (m; CH=CH), 125.19 (m; CH=CH), 124.77 (s; pyr), 109.93 (m; Ar_F-C, C_q), 48.97 (s; CH_3-N). $^{19}F\{^1H\}$ NMR (300 MHz, $CDCl_3$): δ (ppm) -139.9 (2F, m, C-F), -149.75 (1F, m, C-F), -161.19 (2F, m, C-F). MS (ES^+) *m/z*: calcd. for $C_{14}H_9F_5N^+$ 286.07; found 285.89. Elemental analysis: found (calcd.): C, 40.74 (40.70); H, 2.47 (2.20); N, 3.30 (3.39). UV/Vis (EtOH): λ_{max}, nm (ε, cm^{-1} M^{-1}) = 319 (43×10^3).

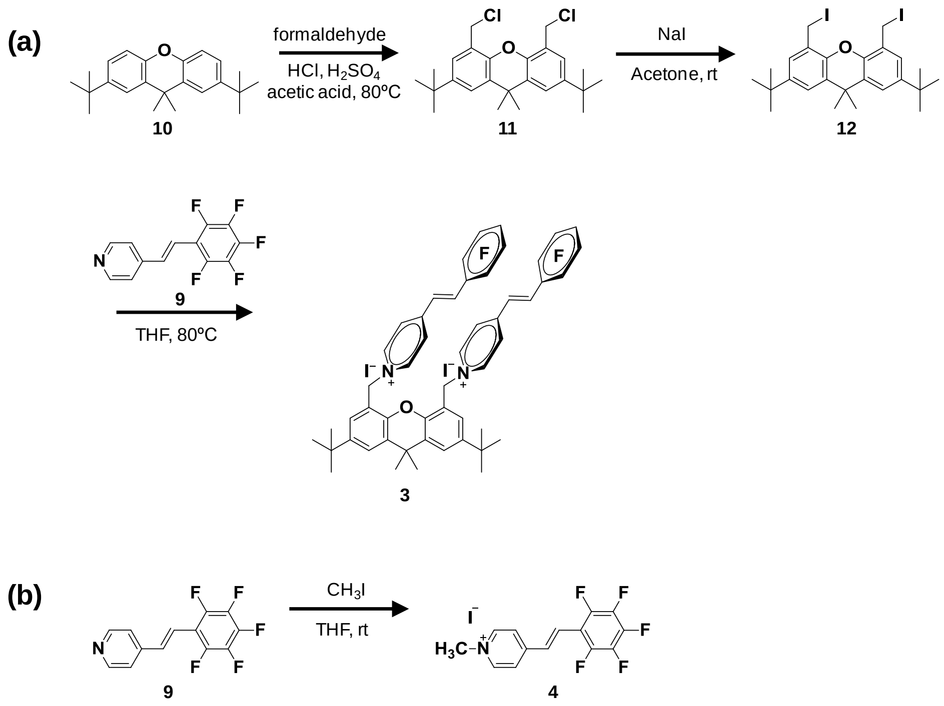

Scheme S3 Synthetic pathways affording compounds (a) **3** and (b) **4**.

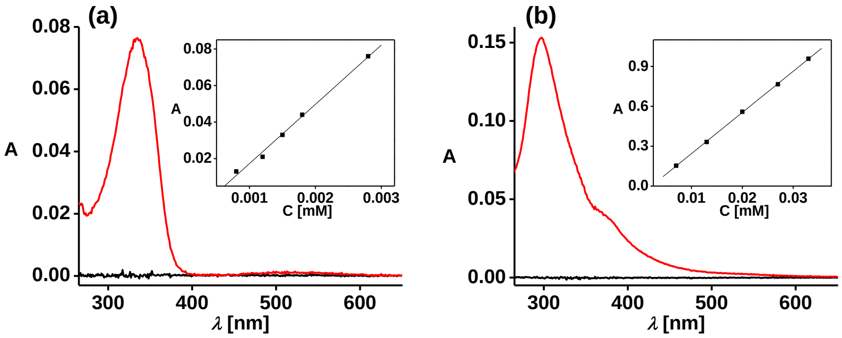

Fig. S2 UV/Vis spectra of compounds (a) **1** (2.8 μM; λ_{max} = 334 nm) and (b) **2** (7.0 μM; λ_{max} = 297 nm) in THF. The baseline was recorded for THF and is shown in black. Insets: a plot of absorbance intensity vs. concentration to determine the molar extinction coefficient of the corresponding compound: the measured data points (black squares); the linear fit of the data points (black solid line). R^2 = 0.994 and 0.999 for insets (a) and (b), respectively.

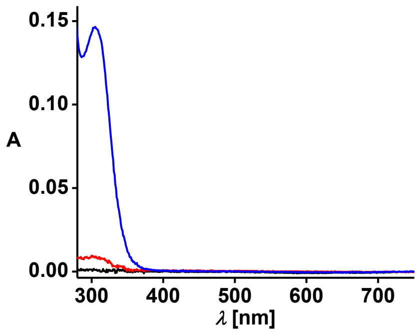

Fig. S3 UV/Vis absorption spectra obtained for ethanol solutions of compound **12**: 1 μM (red) and 20 μM (blue); λ_{max} = 304 nm. The baseline was recorded for ethanol and is shown in black.

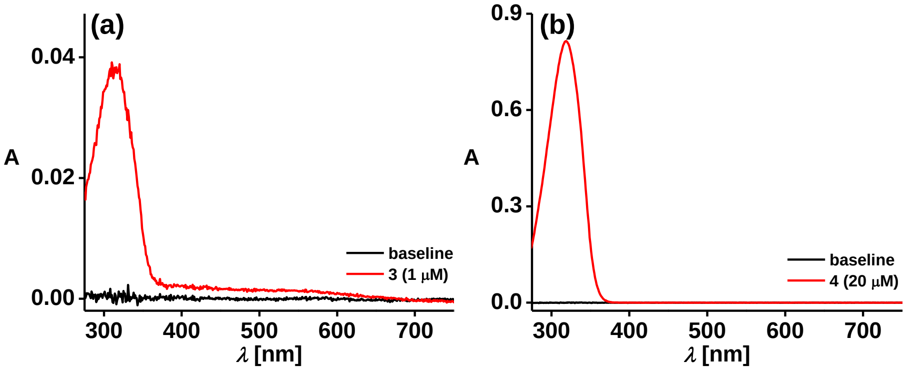

Fig. S4 UV/Vis spectra obtained for ethanol solutions of (a) **3** (1 μM; λ_{max} = 315 nm) and (b) **4** (20 μM; λ_{max} = 320 nm). The baseline was recorded for ethanol and is shown in black. No significant change was observed for (a) after subtracting the absorbance spectrum of compound **12** in the relevant concentration.

Formation of monolayers M1 and M2. Quartz and silicon (100) substrates were functionalized with monolayers **M1** and **M2** under argon and with the exclusion of light. Standard cannula techniques were used to transfer the solutions. The freshly cleaned substrates were placed in a teflon sample holder and immersed in a dry THF solution of compounds **1** (0.2 mM) or **2** (0.2 mM). The reaction vessels were heated 16 h at 80°C. After attaining rt, the slides were sonicated in dry THF (4 × 5 min) under argon. Subsequently, the slides were sonicated in acetone and ethanol (5 min each) and then dried under a stream of N_2. The functionalized substrates were stored under air with the exclusion of light.

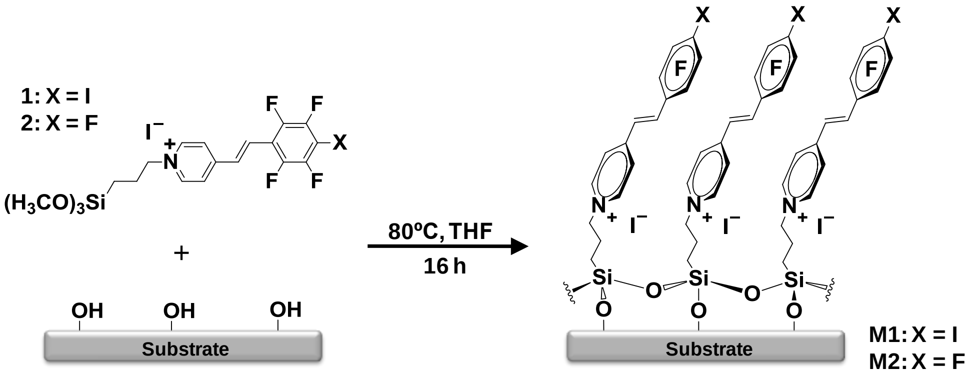

Scheme S4 Schematic representation of the formation of monolayers **M1** and **M2** on silicon (100) and quartz substrates.

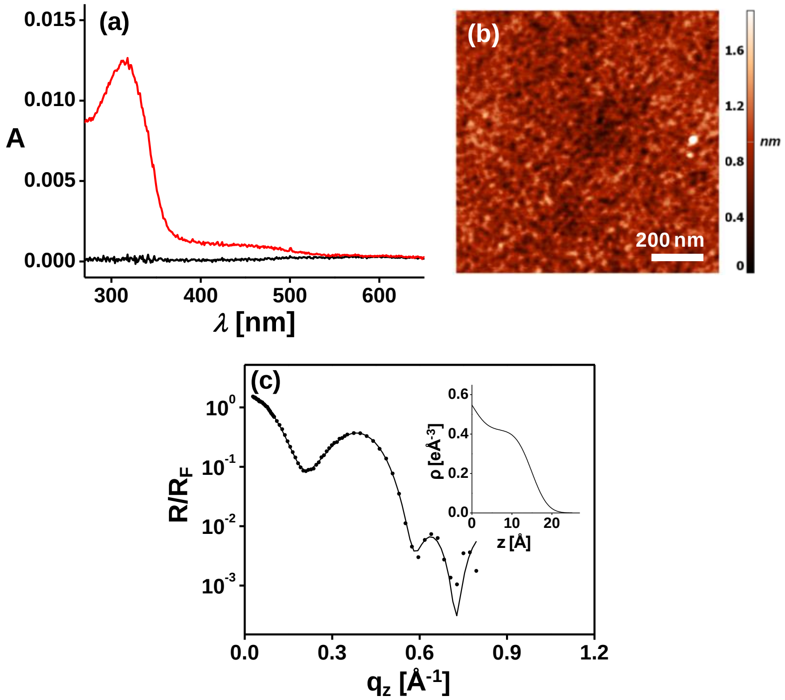

Fig. S5 (a) UV/Vis spectra of monolayer **M2** (λ_{max} = 315 nm) assembled on quartz substrates (red). The baseline was recorded for bare quartz and is shown in black. (b) Representative tapping-mode AFM image **M2** assembled on a silicon substrate. The scan area is 1 μm × 1 μm for which R_q = 0.2 nm. (c) Synchrotron XRR data (black dots) and fit (solid black line) for **M2** assembled on a silicon substrate. Inset: XRR-derived electron density profile of **M2**.

Table S3 XPS elemental ratios for monolayers **M1** and **M2** at θ = 0°.

Elemental ratio[a]	**M1**	**M2**	Expected ratio
C_F/F	1.1	0.9	1 (**M1**, **M2**)
F/N	3.3	5.1	4 (**M1**), 5 (**M2**)
F/I	6.1	---	4 (**M1**, **M2**)
N/I	1.9	---	1 (**M1**, **M2**)

[a] The fluorine and iodine signals decrease over time under the X-ray beam (see Fig. S6). The counter ion is not detected for either of the monolayers.

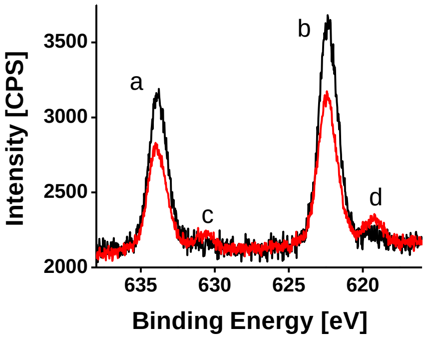

Fig. S6 XPS binding energies for I $3d_{3/2}$ (point a) and I $3d_{5/2}$ (point b) measured for monolayer **M1** at time *t* (black line) and time *t* + 3 min (red line) at $\theta = 0°$. A signal (points c and d, red line) indicating the formation of reduced iodine develops in time at lower binding energies, as the main iodine signal decreases.

Alkyl-CN functionalization of the AFM tips. Freshly cleaned silicon substrates and AFM tips were immersed in a dry pentane solution of 11-cyanoundecyltrichlorosilane (1.0 mM) for 45 min in an N_2-filled glove box (H_2O and O_2 levels <2 ppm). Subsequently, the substrates were washed (5×) with dry pentane under N_2. Then, the substrates were sequentially sonicated (5 min) in pentane and 2-propanol. The slides and tips were then carefully dried under a stream of N_2 and stored under vacuum until use.

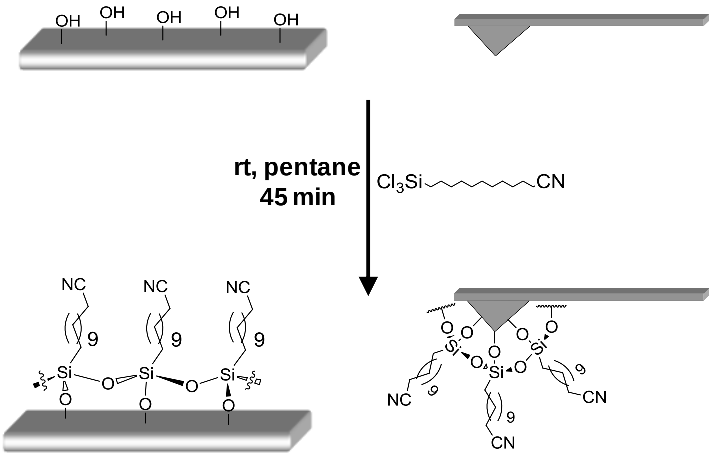

Scheme S5 Schematic representation of alkyl-CN functionalization of a silicon AFM tip and a flat silicon substrate.

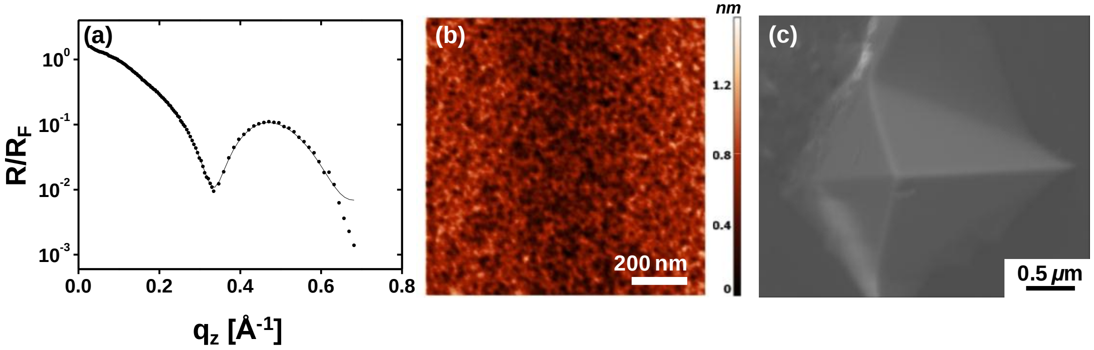

Fig. S7 (a) Synchrotron XRR data (black dots) and fit (solid black line) of an alkyl-CN monolayer assembled on a silicon (100) substrate. (b) Tapping-mode AFM image of an alky-CN monolayer assembled on a silicon substrate. For the 1 μm × 1 μm scan area, R_q = 0.2 nm. (c) Representative SEM image of an 11-cyanoundecyltrichlorosilane-modified AFM tip.

References

(S1) C. B. Aakeroy, N. Schulthesis, J. Desper and C. Moore, *CrystEngComm* **2007**, *9*, 421.

(S2) E. D. Lorance, W. H. Kramer and I. R. Gould, *J. Am. Chem. Soc.* **2002**, *124*, 15225.

(S3) Gaussian 09, Revision C.01, M. J. Frisch, G. W. Trucks, H. B. Schlegel, G. E. Scuseria, M. A. Robb, J. R. Cheeseman, G. Scalmani, V. Barone, B. Mennucci, G. A. Petersson, H. Nakatsuji, M. Caricato, X. Li, H. P. Hratchian, A. F. Izmaylov, J. Bloino, G. Zheng, J. L. Sonnenberg, M. Hada, M. Ehara, K. Toyota, R. Fukuda, J. Hasegawa, M. Ishida, T. Nakajima, Y. Honda, O. Kitao, H. Nakai, T. Vreven, J. A. Montgomery, J. E. Peralta, F. Ogliaro, M. Bearpark, J. J. Heyd, E. Brothers, K. N. Kudin, V. N. Staroverov, R. Kobayashi, J. Normand, K. Raghavachari, A. Rendell, J. C. Burant, S. S. Iyengar, J. Tomasi, M. Cossi, N. Rega, N. J. Millam, M. Klene, J. E. Knox, J. B. Cross, V. Bakken, C. Adamo, J. Jaramillo, R. Gomperts, R. E. Stratmann, O. Yazyev, A. J. Austin, R. Cammi, C. Pomelli, J. W. Ochterski, R. L. Martin, K. Morokuma, V. G. Zakrzewski, G. A. Voth, P. Salvador, J. J. Dannenberg, S. Dapprich, A. D. Daniels, Ö. Farkas, J. B. Foresman, J. V. Ortiz, J. Cioslowski and D. J. Fox, Gaussian, Inc., Wallingford CT, 2009.

(S4) Y. Zhao and D. G. Truhlar, *Theor. Chem. Acc.* **2008**, *120*, 215.

(S5) S. Kozuch and J. M. L. Martin, unpublished work.

(S6) a) F. Jensen, *J. Chem. Phys.* **2001**, *115*, 9113; b) F. Jensen, *J. Chem. Phys.* **2002**, *116*, 7372; c) F. Jensen, *J. Chem. Phys.* **2004**, *121*, 3463; c) F. Jensen, *J. Chem. Phys.* **2002**, *117*, 9234; d) T. H. Dunning, *J. Chem. Phys.* **1989**, *90*, 1007; e) J. M. L. Martin and A. Sundermann, *J. Chem. Phys.* **2001**, *114*, 3408.

(S7) S. Kozuch and J. M. L. Martin, *Phys. Chem. Chem. Phys.* **2011**, *13*, 20104.

(S8) a) J. P. Perdew, K. Burke and M. Ernzerhof, *Phys. Rev. Lett.* **1996**, *77*, 3865. b) J. P. Perdew, K. Burke and M. Ernzerhof, *Phys. Rev. Lett.* **1997**, *78*, 1396. c) C. Adamo and V. Barone, *J. Chem. Phys.* **1999**, *110*, 6158.

(S9) a) S. Grimme, *J. Chem. Phys.* **2003**, *118*, 9095. b) Á. Szabados, *J. Chem. Phys.* **2006**, *125*, 214105.

(S10) C. Møller and M. S. Plesset, *Phys. Rev.* **1934**, *46*, 618-622.

(S11) a) S. Grimme, *J. Comput. Chem.* **2006**, *27*, 1787. b) T. Schwabe and S. Grimme, *Phys. Chem. Chem. Phys.* **2007**, *9*, 3397. c) T. Schwabe, S. Grimme, *Acc. Chem. Res.* **2008**, *41*, 569. d) S. Grimme, J. Antony, S. Ehrlich and H. Krieg, *J. Chem. Phys.* **2010**, *132*, 154104.

(S12) S. Grimme, S. Ehrlich and L. Goerigk, *J. Comput. Chem.* **2011**, *32*, 1456.

(S13) a) E. R. Johnson, A. D. Becke, *J. Chem. Phys.* **2005**, *123*, 024101. b) A. D. Becke and E. R. Johnson, *J. Chem. Phys.* **2005**, *122*, 154104. c) E. R. Johnson, A. D. Becke, *J. Chem. Phys.* **2006**, *124*, 174104.

(S14) a) A. V. Marenich, C. J. Cramer and D. G. Truhlar, *J. Chem. Phys. B* **2009**, *113*, 6378. b) J. Tomasi, B. Mennucci and R. Cammi, *Chem. Rev.* **2005**, *105*, 2999. c) M. Cossi, G. Scalmani, N. Rega and V. Barone, *J. Chem. Phys.* **2002**, *117*, 43.

(S15) a) A. V. Marenich, S. V. Jerome, C. J. Cramer and D. G. Truhlar, *J. Chem. Theor. Comput.* **2012**, *8*, 527. b) A. V. Marenich, C. J. Cramer and D. G. Truhlar, CM5PAC, University of Minnesota, Minneapolis, **2011**. c) F. L. Hirshfeld, *Theoret. Chim. Acta* **1977**, *44*, 129. d) J. P. Ritchie, *J. Am. Chem. Soc.* **1985**, *107*, 1829. e) J. P. Ritchie and S. M. Bachrach, *J. Comp. Chem.* **1987**, *8*, 499.

(S16) E. R. Johnson, S. Keinan, P. Mori-Sánchez, J. Contreras-García, A. J. Cohen and W. Yang, *J. Am. Chem. Soc.* **2010**, *132*, 6498.

(S17) a) R. Krishnan, J. S. Binkley, R. Seeger and J. A. Pople, *J. Chem. Phys.* **1980**, *72*, 650. b) Glukhovstev, M.N.; Pross, A.; McGrath, M.P.; Radom, L. *J. Chem. Phys.* **1995**, *103*, 1878.

(S18) E. Massarani, D. Nardi, L. Mauri and G. Cavallini, *Farmaco, Ed. Sci.* **1963**, *18*, 582.

XYZ coordinates of the optimized structures

Structure **5**

Standard orientation:

Center Number	Atomic Number	Atomic Type	Coordinates (Angstroms)		
			X	Y	Z
1	6	0	0.165661	1.344927	0.000123
2	6	0	1.543249	1.255534	0.000081
3	6	0	2.168894	0.020208	0.000006
4	6	0	1.369011	-1.110805	-0.000094
5	6	0	-0.008992	-1.008037	-0.000073
6	6	0	-0.664006	0.222351	0.000064
7	53	0	4.240914	-0.128845	-0.000007
8	9	0	-0.378455	2.562035	0.000214
9	9	0	2.255366	2.375374	0.000192
10	9	0	1.912824	-2.321980	-0.000187
11	9	0	-0.705808	-2.143737	-0.000170
12	6	0	-2.110584	0.420962	0.000097
13	1	0	-2.401365	1.462522	0.000255
14	6	0	-3.063937	-0.515662	-0.000069
15	1	0	-2.802628	-1.563823	-0.000216
16	6	0	-4.504375	-0.236384	-0.000105
17	6	0	-5.398536	-1.303979	0.000432
18	6	0	-5.055126	1.045328	-0.000545
19	6	0	-6.762673	-1.053851	0.000482
20	1	0	-5.034159	-2.322641	0.000814
21	6	0	-6.430800	1.188041	-0.000451
22	1	0	-4.434532	1.929858	-0.000987
23	7	0	-7.285660	0.166509	0.000041
24	1	0	-7.466602	-1.877667	0.000900
25	1	0	-6.871601	2.177947	-0.000845

Pentanenitrile

Standard orientation:

Center Number	Atomic Number	Atomic Type	Coordinates (Angstroms)		
			X	Y	Z
1	7	0	3.153210	-0.558240	0.000057
2	6	0	2.158710	0.010418	-0.000017
3	6	0	0.875422	0.708657	-0.000049
4	1	0	0.840185	1.355242	0.877803
5	1	0	0.840195	1.355248	-0.877895
6	6	0	-0.311700	-0.257879	-0.000055
7	1	0	-0.247030	-0.906077	0.875534
8	1	0	-0.247134	-0.905920	-0.875766
9	6	0	-1.640788	0.484862	0.000075
10	1	0	-1.688375	1.137547	-0.875096
11	1	0	-1.688321	1.137333	0.875408
12	6	0	-2.829288	-0.466570	-0.000005
13	1	0	-2.811546	-1.109419	0.880329
14	1	0	-3.773010	0.076040	0.000063
15	1	0	-2.811569	-1.109240	-0.880471

6

Standard orientation:

Center Number	Atomic Number	Atomic Type	Coordinates (Angstroms)		
			X	Y	Z
1	6	0	1.289186	1.305556	-0.069198
2	6	0	2.667004	1.265153	-0.012629
3	6	0	3.333949	0.049868	0.038922
4	6	0	2.577661	-1.114887	0.035042
5	6	0	1.200229	-1.064830	-0.020162
6	6	0	0.506929	0.146264	-0.076315
7	53	0	5.399998	-0.024936	0.115138
8	9	0	0.692553	2.492896	-0.120871
9	9	0	3.337236	2.404620	-0.010165
10	9	0	3.165056	-2.298777	0.082719
11	9	0	0.534798	-2.216001	-0.023008
12	6	0	-0.933954	0.286457	-0.152052
13	1	0	-1.257204	1.317975	-0.206285
14	6	0	-1.860361	-0.686763	-0.158872
15	1	0	-1.573233	-1.724630	-0.092799
16	6	0	-3.286945	-0.438142	-0.248635
17	6	0	-4.170160	-1.526998	-0.186189
18	6	0	-3.866530	0.832060	-0.406530
19	6	0	-5.522911	-1.336075	-0.277094
20	1	0	-3.791391	-2.531646	-0.067720
21	6	0	-5.224666	0.964681	-0.493321
22	1	0	-3.266774	1.726503	-0.471485
23	7	0	-6.041073	-0.105420	-0.435474
24	1	0	-6.232784	-2.149112	-0.231228
25	1	0	-5.707842	1.922794	-0.618266
26	6	0	-7.507794	0.083991	-0.467472
27	1	0	-7.711109	0.926319	-1.126378
28	1	0	-7.937838	-0.807442	-0.920416
29	6	0	-8.070313	0.321643	0.926100
30	1	0	-7.591785	1.202140	1.359315
31	1	0	-7.813921	-0.527655	1.562229
32	6	0	-9.580618	0.509721	0.871606
33	1	0	-9.980749	0.673072	1.869019
34	1	0	-9.848050	1.369704	0.258477
35	1	0	-10.070735	-0.369332	0.454279

7

Standard orientation:

Center Number	Atomic Number	Atomic Type	Coordinates (Angstroms)		
			X	Y	Z
1	6	0	2.812548	1.289194	-0.010404
2	6	0	4.188997	1.250075	0.072179
3	6	0	4.827488	0.021328	0.141749
4	6	0	4.084099	-1.150658	0.128521
5	6	0	2.708945	-1.084447	0.045613
6	6	0	2.025682	0.132187	-0.027265
7	9	0	2.225074	2.478339	-0.077357
8	9	0	4.895238	2.363941	0.084637
9	9	0	4.694902	-2.318212	0.194782
10	9	0	2.038774	-2.230755	0.035052
11	6	0	0.585725	0.279508	-0.124532
12	1	0	0.268164	1.312868	-0.177482
13	6	0	-0.344809	-0.688636	-0.150492
14	1	0	-0.063986	-1.728484	-0.089161
15	6	0	-1.770026	-0.433395	-0.254559
16	6	0	-2.656776	-1.520029	-0.215225

```
   17      6       0    -2.343541   0.840410   -0.402368
   18      6       0    -4.008183  -1.323520   -0.316336
   19      1       0    -2.282554  -2.527425   -0.106004
   20      6       0    -3.700617   0.978662   -0.500157
   21      1       0    -1.740456   1.733741   -0.449694
   22      7       0    -4.520718  -0.089310   -0.463049
   23      1       0    -4.720962  -2.134839   -0.287597
   24      1       0    -4.179671   1.939853   -0.617177
   25      6       0    -5.986892   0.105147   -0.502185
   26      1       0    -6.183271   0.959061   -1.148129
   27      1       0    -6.416502  -0.777335   -0.972707
   28      6       0    -6.557192   0.321213    0.891828
   29      1       0    -6.079423   1.193651    1.341876
   30      1       0    -6.305823  -0.538734    1.515582
   31      6       0    -8.066819   0.512835    0.831908
   32      1       0    -8.471993   0.661915    1.829499
   33      1       0    -8.329524   1.382421    0.230393
   34      1       0    -8.556228  -0.358900    0.398753
   35      9       0     6.136621  -0.034631    0.221058
 ---------------------------------------------------------------------
```

8

```
                  Standard orientation:
 ---------------------------------------------------------------------
 Center     Atomic      Atomic             Coordinates (Angstroms)
 Number     Number       Type             X           Y           Z
 ---------------------------------------------------------------------
    1      6       0     0.820170   1.337691    0.044707
    2      6       0    -0.554780   1.298053   -0.048008
    3      6       0    -1.233310   0.087577   -0.080987
    4      6       0    -0.475824  -1.075673   -0.014599
    5      6       0     0.898562  -1.032962    0.076394
    6      6       0     1.598564   0.176334    0.108782
    7     53       0    -3.306234   0.009036   -0.240738
    8      9       0     1.423264   2.524397    0.072444
    9      9       0    -1.215873   2.444009   -0.106797
   10      9       0    -1.063961  -2.262392   -0.039821
   11      9       0     1.559269  -2.187242    0.134201
   12      6       0     3.035167   0.310797    0.202738
   13      1       0     3.364836   1.341725    0.223553
   14      6       0     3.957647  -0.667686    0.255134
   15      1       0     3.663525  -1.705120    0.223890
   16      6       0     5.381434  -0.425067    0.343438
   17      6       0     6.259672  -1.521534    0.323334
   18      6       0     5.971338   0.846689    0.456459
   19      6       0     7.612572  -1.336444    0.406237
   20      1       0     5.874282  -2.527287    0.241668
   21      6       0     7.329610   0.973022    0.537482
   22      1       0     5.377280   1.746609    0.489459
   23      7       0     8.140169  -0.103803    0.517611
   24      1       0     8.316873  -2.155413    0.390228
   25      1       0     7.819334   1.931776    0.627272
   26      6       0     9.606996   0.076358    0.533199
   27      1       0     9.821000   0.946523    1.151312
   28      1       0    10.034919  -0.796119    1.023691
   29      6       0    10.163123   0.247157   -0.872841
   30      1       0     9.686233   1.109775   -1.342270
   31      1       0     9.897810  -0.628121   -1.468865
   32      6       0    11.674628   0.428726   -0.836761
   33      1       0    12.069040   0.549111   -1.842519
   34      1       0    11.950953   1.311519   -0.260986
   35      1       0    12.163147  -0.434972   -0.386746
   36      7       0    -6.206797  -0.170864   -0.545299
   37      6       0    -7.334954  -0.276356   -0.707617
   38      6       0    -8.777711  -0.401313   -0.886766
   39      1       0    -9.060800   0.193021   -1.756480
```